

12-15-2014

Poly-3-hexylthiophene Nanorods as A Donor for Organic Photovoltaics

Dharmesh Patel

Western Kentucky University, dharmesh.patel1086@topper.wku.edu

Follow this and additional works at: http://digitalcommons.wku.edu/stu_hon_theses



Part of the [Chemistry Commons](#)

Recommended Citation

Patel, Dharmesh, "Poly-3-hexylthiophene Nanorods as A Donor for Organic Photovoltaics" (2014). *Honors College Capstone Experience/Thesis Projects*. Paper 509.
http://digitalcommons.wku.edu/stu_hon_theses/509

This Thesis is brought to you for free and open access by TopSCHOLAR®. It has been accepted for inclusion in Honors College Capstone Experience/Thesis Projects by an authorized administrator of TopSCHOLAR®. For more information, please contact topscholar@wku.edu.

POLY-3-HEXYLTHIOPHENE NANORODS AS A DONOR
FOR ORGANIC PHOTOVOLTAICS

A Capstone Experience/Thesis Project

Presented in Partial Fulfillment of the Requirements for

the Degree Bachelor of Science with

Honors College Graduate Distinction at Western Kentucky University

By

Dharmesh Patel

Western Kentucky University
2014

CE/T Committee:

Dr. Hemali Rathnayake, Advisor

Dr. Chad Snyder

Dr. Gordon Baylis

Approved by

Advisor
Department of Chemistry

Copyright by
Dharmesh Jashvantbhai Patel
2014

ABSTRACT

Poly-3-hexylthiophene functionalized silsesquioxane nanorods (P3HT-NRs) were prepared by direct hydrolysis and condensation of P3HT-silane precursor using the modified Stöber method. The silane precursor was stirred in a mixture of two solvents in the presence of a base under room temperature for three different reaction times. The size, shape, and morphology of these novel nanostructures were visualized using the transmission electron microscope (TEM) and scanning electron microscope (SEM). The composition of the P3HT-NRs was confirmed by FTIR and its silane by proton NMR. Future work will focus on evaluating photovoltaic performance of these nanorods as a donor for organic photovoltaics.

Keywords: P3HT, Silsesquioxane, Nanostructures, OPVs, Photovoltaic, Stöber method

Dedicated to my friends and family for always being there for me, and supporting me through the good and rough times. Thanks for all your support in helping me get this far.

ACKNOWLEDGEMENT

I am very grateful of having Dr. Hemali Rathnayake, as my research advisor. I would like to thank her for her time, effort and dedication in helping me complete this project. I really appreciate her determinations in helping understand the chemistry behind organic solar cells. She really took the time and effort to help understand how certain reactions work, and how to interpret the data after analysis. Her determination and motivation towards me as her student has certainly shaped me into the scholar I am today. I would also like to thank my committee – Dr. Chad Snyder and Dr. Gordon Baylis for their support and encouragement. I would like to thank Dr. John Andersland for his enormous help with TEM and SEM support.

I would like to acknowledge the financial support from WKU office of research, Kentucky Commercialization Funds from KSEF, Honors Development Grant [HDG] from Honors College at WKU, and the SGA for the Student development grant. Last but no least, I would like to thank the Department of Chemistry for their support and making it possible for me to attend regional and national conferences to present my research.

Finally, I would like to thank my friends and family for their enormous support and encouragement they have given me to complete my undergraduate thesis. It has truly been a worthwhile experience working in Dr. Rathnayake's research lab.

VITA

December 6, 1991.....Born – Kisumu, Kenya

2008.....St. Andrew’s School, Turi, Mola, Kenya

2010.....Brookhouse International School, Nairobi, Kenya

2013.....Kentucky Academy of Sciences, Morehead, KY
Oral Presentation

2014.....Became an ACS Member

2014.....ACS National Meeting, Dallas, TX,
Poster Presentation

2014.....Kentucky Honors Roundtable,
Bowling Green, KY, Oral Presentation

2014.....Kentucky Academy of Sciences,
Lexington, KY, Poster Presentation

2015.....Poster at the Capitol, Poster Presentation

2015.....ACS National Meeting, Denver, CO,
Poster Presentation

FIELDS OF STUDY

Major Field 1: Biochemistry

Major Field 2: Chemistry

TABLE OF CONTENTS

	<u>Page</u>
Abstract.....	ii
Dedication.....	iii
Acknowledgement.....	iv
Vita.....	v
List of Figures.....	vii
List of Schemes.....	viii
List of Tables.....	ix
Chapters:	
1. Introduction.....	1
I. Organic Photovoltaic.....	2
II. Types of OPVs.....	4
2. Research Objective and Project Goals.....	11
3. Experimental Methods.....	13
4. Results and Discussion.....	17
I. Synthesis and structural characterization.....	17
II. Morphology.....	22
5. Conclusion.....	26
Bibliography.....	27

LIST OF FIGURES

<u>Figure</u>	<u>Page</u>
1.1 Single layer OPV.....	4
1.2 Bilayer OPV.....	5
1.3 Bulk heterojunction OPV.....	7
1.4 Donor Materials for OPV.....	8
1.5 Acceptor Material for OPV.....	9
4.1 P3HT Nanorods TEM.....	22
4.2 P3HT Nanorods TEM.....	22
4.3 IR analysis of P3HR-Si.....	23
4.4 P3HT Nanorods TEM.....	23
4.5 P3HT Nanorods TEM.....	23
4.6 P3HT Nanorods TEM.....	24
4.7 P3HT Nanorods TEM.....	24
4.8 P3HT Nanorods TEM.....	24
4.9 P3HT Nanorods TEM.....	24
4.10 P3HT Nanorods TEM.....	24
4.11 P3HT Nanorods TEM.....	24
4.12 P3HT Nanorods TEM.....	25
4.13 P3HT Nanorods TEM.....	25

LIST OF SCHEMES

<u>Schemes</u>	<u>Page</u>
4.1 Preparation of P3HT Nanorods using the modified Stöber Method.....	17

LIST OF TABLES

<u>Tables</u>	<u>Page</u>
4.1 Reaction conditions for synthesizing P3HT Nanorods.....	19

CHAPTER 1

INTRODUCTION

The harnessing of solar energy has been achieved using a wide range of technologies such as: artificial photosynthesis, solar heating, and photovoltaics among many others. ^{[1][2]} The artificial photosynthesis utilizes the photoelectric effect where as the photovoltaics utilizes the photovoltaic effect. The difference between the two effects is that, in photoelectric electrons are emitted from the surface of the material due to the absorption of the electromagnetic spectrum, where as in photovoltaic the electrons are transferred from the valence band to the conduction band of the material. ^[3] Today, solar energy offers mankind with infinite energy resource that is relatively abundant around the globe. Its availability is considered to be greater in countries closer to the equator that have sunlight all year round, hence the solar energy can be greatly utilized. ^[1]

The advantages and unlimited access of solar energy has led to a total global capacity of 139 gigawatts (GW), while Germany being the largest producer it has the capability of subsidizing 6% to its national energy demand. ^[4] The challenges faced in lowering the electricity costs has led to the research of utilizing organic elements for organic photovoltaic solar cells (OPVs) as an alternative to the silicon based solar cells. The organic based solar cells are the future focus for making: cheaper, recyclable, low cost solar panels to surpass the power conversion efficiency of the silicon based.

By utilizing the renewable resources, there will be a cost reduction in electricity

as well as achieving sustainable energy. ^[5] Upon achieving a power conversion efficiency of approximately more than 10%, there are still questions about its efficiency limitations, long-term reliability, and its lifetime performance that need to be addressed. ^[6]

My research goal is to prepare novel nanostructures that will serve as a donor material for the active layer, which will improve the power conversion efficiency of the organic-based solar cells. This thesis will serve as a mode to better understand my research and the work I have done towards achieving this goal. The thesis is organized as follows: In the first part, a general introduction will be given on organic photovoltaics (OPVs), and different types of OPVs. In the second part, the incorporation of poly-3-hexylthiophene nanorods (P3HT-NRs) into organic photovoltaic (OPV) cells will be discussed for future performance evaluation.

I. Organic Photovoltaic (OPV) Cells

As previously discussed, OPVs help subsidize the high costs of energy, and creating sustainable energy. The solar cells consist of a thin film conjugated organic polymers that absorb light and transfer charge in order to produce electricity. The conjugated system formed in the OPVs is due to the alternating single and double bonds on the covalently bonded carbon atoms. ^[7]

Due to the conjugated system of the organic polymers, a delocalized π orbital and π^* antibonding orbital are formed due to the p_z orbital. Where the delocalized π orbital is the highest occupied molecular orbital (HOMO), and π^* antibonding orbital is the lowest unoccupied molecular orbital (LUMO). The charge difference of the electron between the

HOMO and LUMO create a band gap that typically ranges from 1-4 electron volts (eV).
[7]

The first silicon solar cell was publically demonstrated in 1954 by the three scientists; Chaplain, Fuller and Pearson at Bell laboratories. [8][9] They got the idea from a French scientist: Edmond Becquerel, who was the first inventor of the photovoltaic cell in 1839. [8][9] Later in 1994 R. N. Marks et al. created the first OPV cell that consisted of poly(p-phenylene vinylene) (PPV) with a thickness between the range of 50-320 nm, which was sandwiched between indium tin oxide (ITO) glass and a cathode (Al, Mg or Ca). [10] Upon exposure to light with an intensity of 0.1 mW/cm^2 , the efficiency of the device came to around 1%. [10] Despite the low power conversion efficiency, the solar cell development has really advanced over the years with new materials being synthesized to improve the efficiency. The ability to control the band gap and electronegativity through the molecular designs of materials has led to the synthesis of conducting polymers with better electron affinities. [11]

Typically, when these materials absorb a photon, the generated excited state is confined to a molecule or a region of a polymer chain. The excited state can be regarded as an electron-hole pair bound together by electrostatic force, otherwise referred to as excitons. [12][13] In OPVs, the excitons are broken up into free electron-hole pairs by effective fields, forming a heterojunction between two different semiconductor materials. [14] These electric fields split the exciton by causing the electron to fall from the conduction band of the electron donor to the conduction band of the electron acceptor.

Therefore, it is crucial that the acceptor material has a conduction band edge that is lower than that of the donor material. ^{[15][16]}

II. Types of OPVs

The single layer OPV is one of the simplest types of organic photovoltaic cell. The cell comprises of three components; indium tin oxide (ITO) glass [electrode 1], organic electronic material, and a layer of magnesium, aluminum or calcium [electrode 2]. For the cell to function, the organic electronic material is sandwiched between the top and bottom layer. The top layer is the high work function metal (ITO coated glass), while the bottom layer is the low work function metal such as (Mg, Al, Ca). ^[17] A schematic representation of the basic structure is illustrated in Figure 1.1.

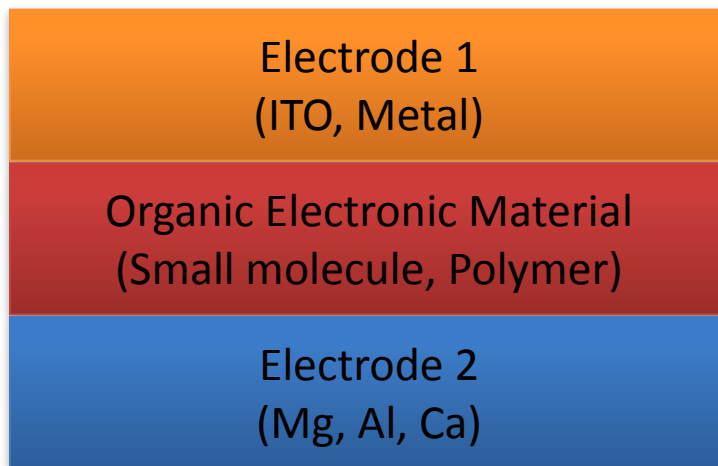


Figure 1.1: A schematic representation of a single layer organic photovoltaic cell.

The difference in work function between the two electrodes generates an electric field in the organic electronic material. Therefore, when the active organic layer is struck

by a photon the electrons will be excited to the LUMO leaving a hole in the HOMO. The exciting of the electrons from LUMO to HOMO results in the formation of the excitons, which then leads to the dissociation of the electron-hole pair as the excitation falls from the excited state to the ground state.^[18] The potential created by the two different electrodes helps separate the exciton pairs, pulling the electrons to the positive electrode and holes to the negative electrode. The single layer OPV has shown low quantum efficiencies (<1%) and low power conversion efficiency [PCE] (<0.1%). A problem with the single layer OPV is that the electric created from the difference between the two conductive electrodes is insufficient in diving the excitons, hence as a result the electrons recombine with the holes before reaching the electrode.^[17]

To overcome the issue of the single layer OPV, an addition if a second organic layer in conjunction with the first organic layer creating a bilayer OPV is depicted in Figure 1.2.

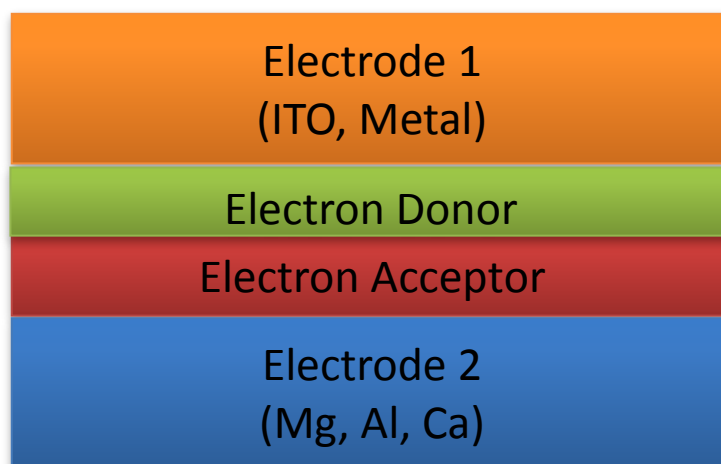


Figure 1.2: A schematic representation of a bilayer organic photovoltaic cell.

A bilayer cell utilizes the same electrodes as the single layer cell; the only difference is that the cell utilizes the electrostatic force generated between the two organic materials that have different electron affinities and ionization energies. The layer with the high electron affinity and ionization energy is the electron acceptor, while the other layer is the electron donor. It is due to the unequal band gap between the two materials that generates a strong electric field to efficiently split the excitons. ^[12]

There is a slight improvement in terms of; quantum efficiency of 6% with a PCE of 1%, but the diffusion length of the excitons in organic electronic material is about 3-40nm. ^[19] To have most of the excitons diffuse to the interface of the polymer layers and split into charge carriers the diffusion length should be same as the thickness of the polymer layer. A typical polymer layer is 100 nm thick for it to actually absorb enough light; therefore at this large thickness only a small fraction of the excitons can reach the heterojunction. ^[12]

To overcome the issue of thickness and diffusion length of the excitons, a combination of the electron donor and electron acceptor, forming a polymer blend is implemented. The combination of the electron donor and electron acceptor, forming a polymer blend is called a bulk heterojunction OPV; depicted in Figure 1.3. ^{[20][21]} The combination of the electron donor and electron acceptor allows the polymer blend length and the exciton diffusion length to be similar; hence the generated excitons can reach the interface and split efficiently. ^[20]

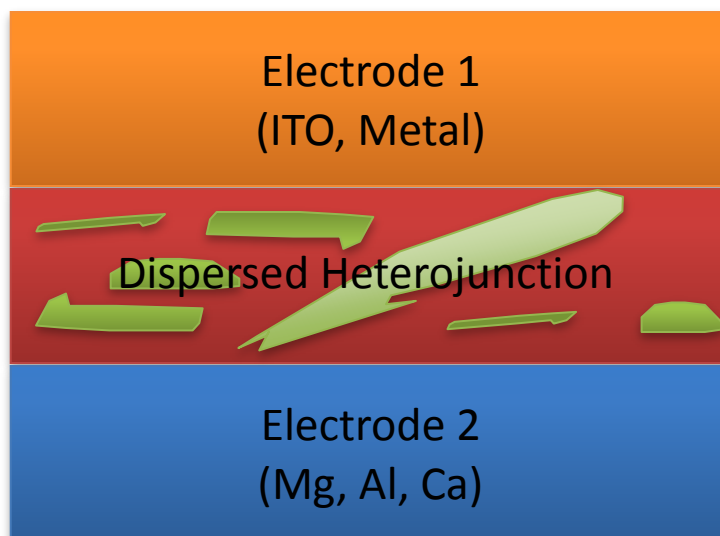


Figure 1.3: A schematic representation of Bulk heterojunction OPV cell.

The disadvantage in this kind of OPV configuration is that the electrons get trapped in the active layer, hence not making it to the electrodes. It is more like spaghetti and meatballs; that is the electrons have a hard time getting through to the electrodes. Numerous advances have been made to minimize the trapping of the electron, and to increase the power conversion efficiencies. An example is the controlled growth heterojunction that provides better control over the positions of the donor-acceptor materials, and eventually leading to higher power conversion efficiency. ^[22]

To date numerous donor and acceptor materials for organic based solar cells have been synthesized; most of which have been incorporated into the active layer of the cell. The most commonly used donor and acceptor materials are Poly (3-hexylthiophene) (P3HT) and phenyl-C61-butyric acid methyl ester (PCBM). The blend of two materials

can achieve a high PCE of approximately 3.5 to 5.0%.^[25] Figure 1.4 shows some of the donor materials that have been synthesized for their application in the active layer blend.

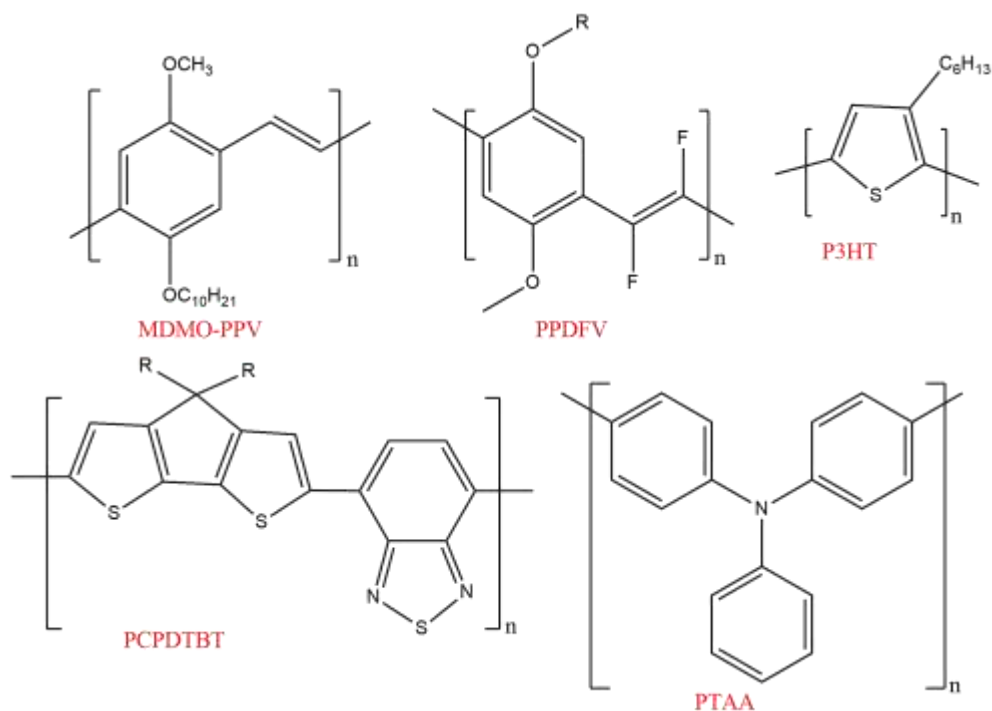


Figure 1.4: Chemical Structure of Donor materials for Organic solar cell.

Despite the synthesis of these donor materials there are still limitations in controlling the morphology, and the ability to transport the hole to the electrode. Figure 1.5 shows some of the acceptor materials available and tested in the active layer of the OPVs along with the donor materials shown previously in Figure 1.4. Considering the several donor and acceptor materials, not a single combination of the material as an active layer is able to obtain over 3% PCE except for P3HT/PCBM and PCPDTBT/PCBM.^[26]

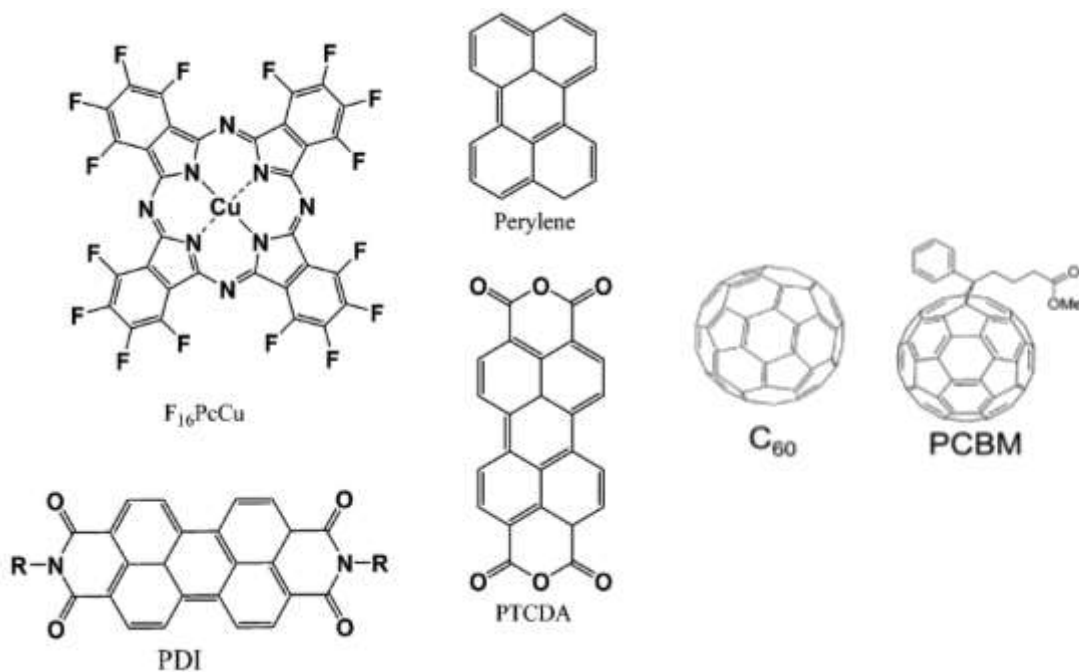


Figure 1.5: Chemical Structure of Acceptor materials for Organic solar cell.

The combination of P3HT (donor material) and PCBM (acceptor material) in the active layer has potential of obtaining a higher PCE than its current achievement if about 3-5%.^[27] The use of P3HT as an electron donor in polymer:fullerene BHJ have shown PCE of up 5%, therefore being able to control the morphology of P3HT derivatives such as P3HT NRs will lead to higher PCE for OPVs.^[27] Rathnayake et al., have recently synthesized P3HT nanoparticles using the modified Stöber method as a donor material for the for OPVs.^[29] The Stöber method, named after Werner Stöber, is used for producing silica nanoparticles. He was the first to synthesize spherical silica particles through the hydrolysis alkyl silicates and condensation of silicic acid in solution, in the presence of a morphological catalyst.^{[23][24]} Later, the Stöber method was slightly

modified by Unger's group to prepare silica sphere in which they utilized cetyltrimethylammonium bromide; since then it has been known as the modified Stöber method. [24]

Rathnayake et al., evaluated the photovoltaic performance of P3HT nanoparticles with PCBM in a 1:1 blend ratio, which resulted in a PCE of 2.5%. [29] Therefore, there is potential in increasing the PCE of OPVs by having P3HT derivatives in the active layer along with PCBM. Therefore, considering the potential of P3HT nanoparticles my research goal is to synthesize P3HT nanorods as a donor for OPVs to achieve high PCE for sustainable energy.

CHAPTER 2

RESEARCH OBJECTIVE AND PROJECT GOALS

Objective:

To create functionalized nanorods derived from poly-3-hexylthiophene as an active donor for organic photovoltaic cells. This donor material comprising of a low band gap, and the ability to control the morphology will be able to provide a higher PCE. The functionalized silsesquioxane P3HT-NRs will be synthesized using the modified Stöber method. ^[23]

Goals:

- Preparation of P3HT-NRs
- Characterization of the P3HT-NRs
- Evaluating photovoltaic performance

Method and Approach

P3HT being the most common compound used for solar cell devices is due to its function as a donor. The P3HT-NRs will be synthesized using the modified Stöber method; a direct hydrolysis and condensation of organotrialkoxysilanes in the presence of catalytic amount of base. ^{[23][24]} The synthesis proceeds for 24-72 hours through a hydrolysis and condensation reaction leading nanorods formation containing Si-O-Si

network.

P3HT nanorods will be prepared by following the modified Stöber method in the presence of a base under two separate conditions. Three different concentrations will be used in each method. One method will run under stirring condition and the other non-stirring condition to compare the morphology of nanostructures. These materials will be characterized using NMR, IR, TEM, and SEM. The chemistry of this modified Stöber method to prepare P3HT-functionalized silsesquioxane nanorods will be discussed in detail in the Results and Discussion section.

Subsequent synthetic methods will be used to prepare the silane precursor, P3HT-SiMe(OC₂H₅)₂ from 2,5-dibromo-3-hexylthiophene. P3HT will be prepared using the Grignard metathesis and Kumada coupling^{[30][31]} followed by carboxylation of chain end to P3HT-COOH through Steglich esterification.^[28] The P3HT-COOH will be coupled with 3-aminopropylmethyldiethoxysilane to yield P3HT-silane, which will be hydrolyzed with a base (ammonium hydroxide) in a solvent mixture of Chloroform and anhydrous ethanol to yield the P3HT-NRs. To produce these nanostructures the mixture will stir for 24, 48 and 72 hours at room temperature.

CHAPTER 3

EXPERIMENTAL METHODS

Materials: 2,5-dibromo-3-hexylthiophene, *tert*-Butylmagnesium chloride (^tBuMgCl) (1.6 M in THF), *n*-Butyllithium (1.6 M in Hexane), 4-(Dimethylamino) pyridine (DMAP), *N,N'*-dicyclohexylcarbodiimide (DCC), anhydrous tetrahydrofuran, dichloro[Bis(1,3-diphenylphosphino)propane] nickel(II) (Ni(dppp)Cl₂), chloroform-*d*, anhydrous ethanol, and chloroform were purchased from Sigma-Aldrich. Ammonium hydroxide (28%) was purchased from Fischer Scientific. 3-aminopropylmethyldiethoxysilane was purchased from Alfa Aesar. All the chemicals were used as purchased from the vendors, unless otherwise specified.

Characterization: Proton NMR spectra were recorded on a 500 MHz Jeol using chloroform-*d* (CDCl₃) as the solvent. FTIR spectra were measured using Perkin-Elmer Spectrum One FT-IR spectrometer equipped with a universal ATR sampling accessory. Transmission electron microscope (TEM) observations were performed on a JEOL 1400CX at 80 keV.

General procedure for the preparation on poly-3-hexylthiophene (P3HT): 2,5-dibromo-3-hexylthiophene (482 mg, 14.78 mmol) was added in a 100 mL three-neck round bottom flask and sealed with a water condenser and septa. The flask was then

flushed with argon and anhydrous THF (30 mL) was injected. $t\text{BuMgCl}$ (14.78 mL, 14.78 mmol) was then injected drop wise into the flask and the mixture was raised to 80°C using an oil bath and refluxed for 2 hours under argon while stirring. Upon addition of $t\text{BuMgCl}$ a resulting yellow solution was observed. The solution was then cooled to room temperature and Ni(dppp)Cl_2 (133 mg, 0.246 mmol) was added and flushed under argon, and a deep red/purple coloration was observed. The reaction was stirred for 30 minutes. Then a second addition of Ni(dppp)Cl_2 (66 mg, 0.123 mmol) was added and let to stir for 30 minutes. The reaction was then quenched with 5 drops of methanol and transferred into a beaker-containing methanol (50 mL). The deep red/purple precipitate was then filtered out using a Büchner funnel and washed with hexane till a clear filtrate was observed. The deep red/purple solid was then dried under vacuum oven to yield 1.8405 grams of P3HT (Yield = 38.2%). $^1\text{H-NMR}$ in CDCl_3 $\{\delta, \text{ppm}\}$: 7.44 (s (weak), 1H, terminal H), 6.97 (s 23H), 6.82 (s (weak, Br), 1H), 2.80 (s (Br), 43H), 1.70-1.33 (m (200H), 0.91 (s, 79H). Molecular weight (MW) of the polymer was determined by $^1\text{H-NMR}$ spectrum with the respect to terminal hydrogen of P3HT polymer chain end and calculated MW = 3905.41 g/mol.

Carboxylic acid terminated poly-3-hexylthiophene: P3HT (500 mg, 0.128 mmol) was added to a 50 mL three neck round bottom flask, sealed with a water condenser and septa. The flask was then flushed with argon and anhydrous THF (30 mL) was injected. The flask was then lowered into a dewar flask and cooled to -78°C using dry ice and acetone.

n-BuLi (0.09 mL) was then injected into the flask drop wise and let to stir for one hour. The solution was then warmed to room temperature and bubbled with CO₂ for 30 minutes and stirred for 30 minutes. CO₂ was bubbled again for another 30 minutes and stirred for 30 minutes. The reaction was the quenched with 1.5 mL of 15% HCL and the precipitate was transferred into a beaker containing methanol (30 mL). The precipitate was then filtered out using a Büchner funnel and washed with hexane till a clear filtrate was observed. The solid was then dried under vacuum oven to yield 0.40g of P3HT-COOH (Yield = 56.4%). ¹H-NMR in CDCl₃ { δ , ppm}: 7.45 (s (weak), 1H), 6.97 (s 30H), 6.82 (s (weak, Br), 1H, terminal H), 2.80 (s (Br), 64H), 1.70-1.33 (m (338H), 0.91 (s, 112H); FT-IR stretching's (cm⁻¹): 3370-3000 (-OH from carboxylic acid), 2923-2854 (alkyl C-H), 1700 (carbonyl, weak), 1625-1509 (aromatic C-C), 819 (S-C). Molecular weight (MW) of the polymer was determined by ¹H-NMR spectrum with the respect to terminal hydrogen of P3HT polymer chain end and calculated MW = 5034.50 g/mol.

Poly-3-hexylthiophene carboxy diethoxymethylsilane (P3HT silane precursor):

Carboxylic acid terminated P3HT (300 mg, 0.0596 mmol), DCC (25 mg), DMAP (20 mg), were all added to a single necked round bottom flask and flushed with argon. Anhydrous THF (30 mL) was then injected into the flask and a purple solution was observed. 3-aminopropylmethyldiethoxysilane (0.05 mL, 40 mg, 0.0655 mmol) was injected into the flask and the reaction was let to stir for 24 hours under inert atmosphere. The reaction was then quenched with hexane (5 drops), and precipitated in hexane (15

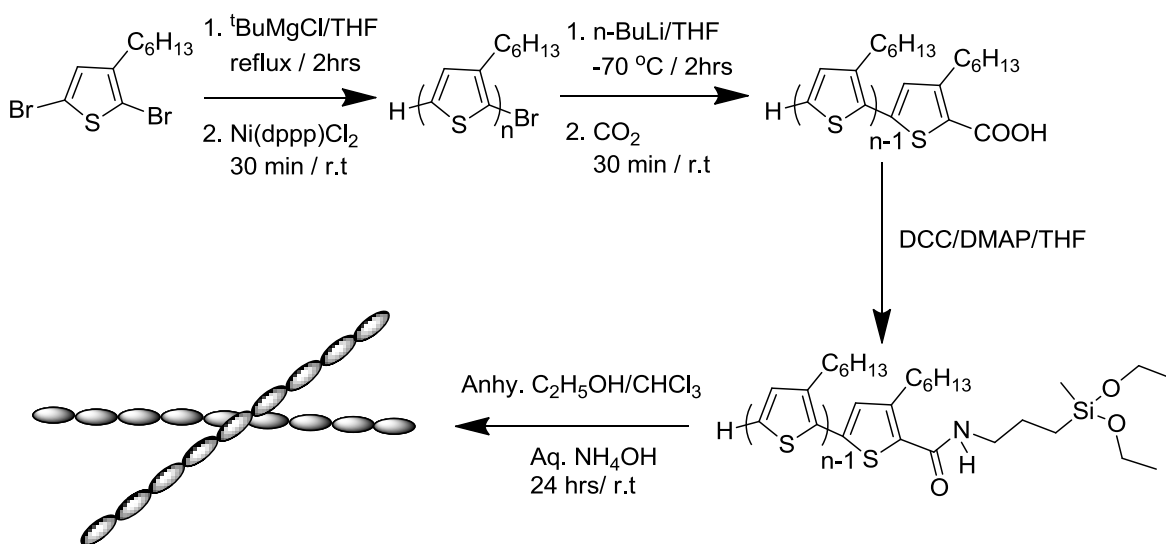
mL). The dark red/purple precipitate was then filtered out using a Büchner funnel. The dark red/purple solid was then dried under vacuum oven to yield 0.14g of P3HT (Yield = 41.0%). $^1\text{H-NMR}$ in CDCl_3 $\{\delta, \text{ppm}\}$: 7.04 (s (weak), 1H), 6.97 (s 19H), 6.82 (s (weak, Br), 1H, terminal H), 2.80 (s (Br), 41H), 1.70-1.34 (m (171H), 0.91 (s, 75H); FT-IR stretching's (cm^{-1}): 3100-3000 (-NH), 2923-2854 (alkyl C-H), 1694 (carbonyl, weak), 1625-1510 (aromatic C-C), 1375-1248 (Si-C), 804 (S-C). Molecular weight (MW) of the polymer was determined by $^1\text{H-NMR}$ spectrum with the respect to terminal hydrogen of P3HT polymer chain end and calculated MW = 5207.83 g/mol.

Typical procedure for the preparation of P3HT-Nanorods: In a vial P3HT silane precursor (20 mg) was dissolved in chloroform (4 mL), anhydrous ethanol (200 proof, 4 mL) was added through the wall, followed by ammonium hydroxide (28%, 0.6 mL) through the wall. A resulting purple mixture was observed and the reaction was let to stir for 24 hours at room temperature. A spot of the sample was then spotted on a carbon coated copper grid, and the solution was then centrifuged yielding a yellowish supernatant and a purple precipitate. The supernatant was decanted and stored in a vial, while the precipitate was let to dry in the vacuum oven. An average size of 600 nm was confirmed for the P3HT-NRs from the TEM.

CHAPTER 4

RESULTS AND DISCUSSION

P3HT functionalized silsesquioxane nanorods were synthesized following the reaction mechanism depicted in scheme 4.1. An approach taken to synthesize these nanostructures was through a modified Stöber method. [23][24]



Scheme 4.1: Preparation of P3HT Nanorods using the modified stöber method with the poly-3-hexylthiophene diethoxysilane precursor.

I. Synthesis and structural characterization

The starting molecule, 2,5-dibromo-3-hexylthiophene is used in a Grignard Metathesis followed by Kumada coupling reaction to yield poly-3-hexylthiophene. [30][31]

The Grignard metathesis (GRIM) method is used to synthesis a Grignard monomer of the

starting material in the presence of t-BuMgCl reagent.^[30] The Grignard monomer in the presence of Ni catalyst undergoes cross coupling reaction to form carbon-carbon bonds.^[31] 2,5-dibromo-3-hexylthiophene dissolved in THF refluxed for 2 hours at 80°C, after the addition of t-BuMgCl and followed by the addition of Ni(dppp)Cl₂ catalyst for cross coupling of the Grignard monomer with the halogen terminated thiophene to yield poly(3-hexylthiophene). The reaction was then quenched and washed with methanol. After washing with methanol followed by washing with hexane, the solid was collected and let to dry in the vacuum oven. The synthesized P3HT was characterized using proton NMR, where the number of repeated thiophene units at 6.98 ppm was determined with respect to the terminal hydrogen at 7.40 ppm. The molecular weight of P3HT was determined to be approximately 3905.41 g/mol.

The P3HT was then carboxylated in the presence of n-BuLi at approximately -78°C for an hour. Once at room temperature, it was bubbled twice with carbon dioxide for 30 minutes and stirred for 30 minutes to yield poly-3-hexylthiophene with a carboxylic group at the chain end. The product was then quenched with 1.5 mL of 15% HCL, followed by washing with methanol and hexane to remove any impurities. The solid was collected and let to dry in vacuum oven over night. The FTIR confirms the successful carboxylation of P3HT from the hydroxyl functional group stretchings at 3370 – 3000 cm⁻¹. P3HT-COOH was also characterized using proton NMR, where the number of repeated thiophene units at 6.98 ppm was determined with respect to the terminal hydrogen at 7.40 ppm. The molecular weight of P3HT was determined to be

approximately 5034.50 g/mol.

The carboxylated P3HT was then coupled with 3-aminopropylmethyldiethoxysilane in the presence of DCC and DMAP using Steglich esterification^[28] to yield poly-3-hexylthiophene diethoxysilane precursor. The product was then washed twice with hexane and solid was collected. The FTIR confirms the successful esterification of P3HT-COOH to P3HT-Si by detecting the presence of the C-Si peak at 1377 cm^{-1} . The peak confirms the presence of the carbon silicon bond. The solid was also characterized using proton NMR, where the number of repeated thiophene units at 6.98 ppm is determined with respect to the terminal hydrogen at 7.40 ppm. The molecular weight of P3HT is determined to be approximately 5207.83 g/mol.

The direct hydrolysis and condensation of the silane precursor using the modified Stöber method is used to yield distinctive nanostructures based on the different base concentration. The stirring and non-stirring condition was implemented in the synthetic method for these novel nanostructures, to determine the best-suited condition. The data obtained from the trial reactions determined that the stirring condition is more favorable for synthesizing these novel nanostructures.

Numerous trials were run using the modified Stöber method for the synthesis of P3HT NRs. The experimental conditions, morphology and particle size distribution data for the trials are reported in Table 4.1.

Table 4.1: Experimental conditions, morphology and particle size distribution of P3HT Nanostructures synthesis.

P3HT-NRs Trials	P3HT Silane precursor (mmol)	NH ₄ OH (aq) (mmol)	Morphology of Nano structures	Nanostructures size distribution
1	1.32×10^{-3}	8.64	Mostly Nano rods, with few nanoparticles	950 ± 50 nm
2	3.84×10^{-3}	11.52	Nanoparticles	200 ± 30 nm
3	3.84×10^{-3}	14.4	Nano ribbons	1.7 ± 0.2 μ m
4	3.84×10^{-3}	8.64	Nanorods	850 ± 30 nm
5	7.43×10^{-3}	8.64	Nanorods	480 ± 20 nm
6	7.43×10^{-3}	11.52	Nanoparticles	100 ± 20 nm
7	7.43×10^{-3}	14.4	No rods	-
8	1.86×10^{-2} 50mg	8.64	Nanorods	2 ± 0.5 μ m
9 (48 hrs)	1.86×10^{-2}	8.64	Nanoparticles	150 ± 20 nm
10 (72 hrs)	1.86×10^{-2}	8.64	Nanoparticles	0.2 ± 0.01 μ m
11	3.84×10^{-3}	8.64	Nanorods	900 ± 20 nm
12 (48 hrs)	3.84×10^{-3}	11.52	Nanoparticles	90 ± 10 nm

As shown in Table 4.1, the moles of P3HT silane used are not the same for all trials as the molecular weight for the silane precursor varied from 2700 to 10000 g/mol. The synthesized P3HT was compared to the commercial P3HT in the preparation of the P3HT-NRs, but the commercial P3HT did not show any nanorods, as the molecular

weight is around 45000 g/mol that is 4.5 times higher than the lab synthesized P3HT.

Trial one shows the reaction conditions for the first functionalized nanorods, where a 1:1 ratio of ethanol to chloroform was used, along with 8.64 mmol ammonium hydroxide to help control the morphology of the nanostructures. The reaction was run for 24 hours under room temperature, and stirring condition. The sizes of the nanorods were confirmed using TEM to be approximately 700 nm. The nanorods were present in the supernatant rather than the solid after centrifugation. There were some nanoparticles present both in the supernatant and the solid.

In trial two, the ratio of chloroform to ethanol was kept constant and the concentration of ammonium hydroxide was reduced to 11.52 M. This resulted in the formation of the nanoparticles with an average particle size of 200 nm. The reaction was run for 24 hours under room temperature, and stirring condition. After centrifugation the nanoparticles were present in the solid. This was confirmed by dissolving the solid in ethanol and chloroform.

For trial three the ratio of chloroform to ethanol was the same but ammonium hydroxide concentration was 14.4 M. The reaction was run for 24 hours under room temperature, and stirring condition. This resulted in the formation of few nanoparticles and nanoribbons.

The nanostructures for Trials 2 and 4 from Table 4.1 are shown in Figures 4.4 and 4.5 respectively. From the TEM images we can evaluate that the change in the number of moles NH_4OH yielded both the nanoparticles and nanoribbons. The same number of

moles was used for trials 5 through 7, which were run under room temperature and non-stirring condition. The number of moles of ammonium hydroxide base for the three trials was varied from 8.64, 11.52, and 14.4 mmol. The number of moles for NH_4OH used for the trials 5, 6, and 7 was 8.64, 11.52, and 14.4 mmol respectively. The TEM images are shown in Figures 4.6 through 4.8.

II. Morphology

As shown in Figure 4.1 and 4.2, the TEM images confirm the successful formation of the P3HT-NRs. The images are for trials 1 and 4 from Table 4.1.

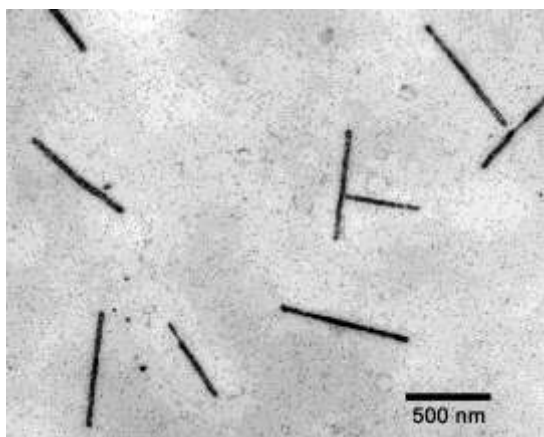


Figure 4.1: Trial 1, P3HT Nanorods
(Scale bar 500 nm)

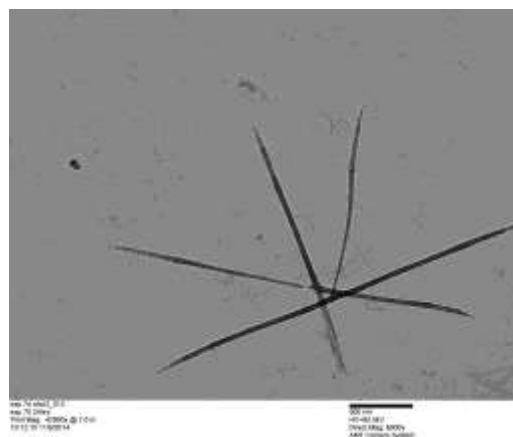


Figure 4.2: Trial 4, P3HT Nanorods
(Scale bar 100 nm)

The composition of P3HT-NRs was confirmed by FTIR and as shown in Figure 4.3, it confirms the composition of the P3HT-NRs with Si-O-Si present at 1072 cm^{-1} and C-Si at 1377 cm^{-1} .

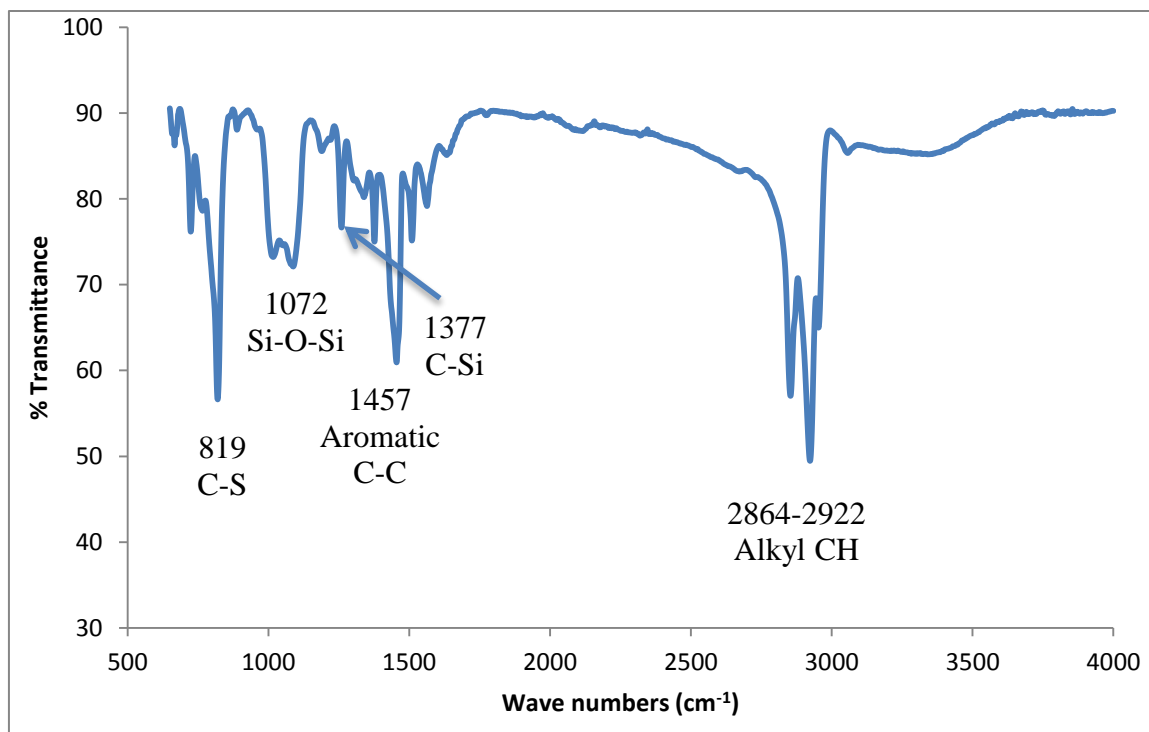


Figure 4.3: FTIR showing the composition of P3HT-NRs.

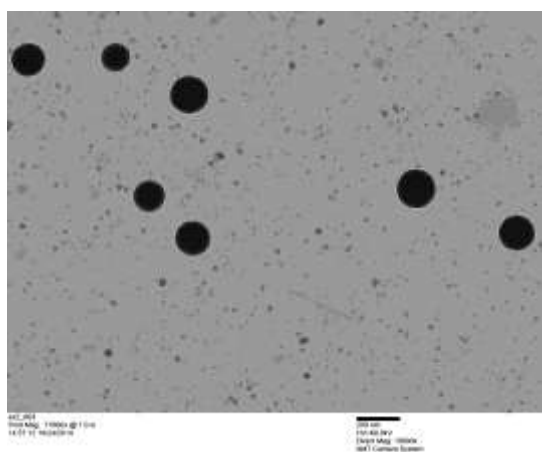


Figure 2.4: Trial 2, P3HT Nanoparticles (Scale bar 200 nm)

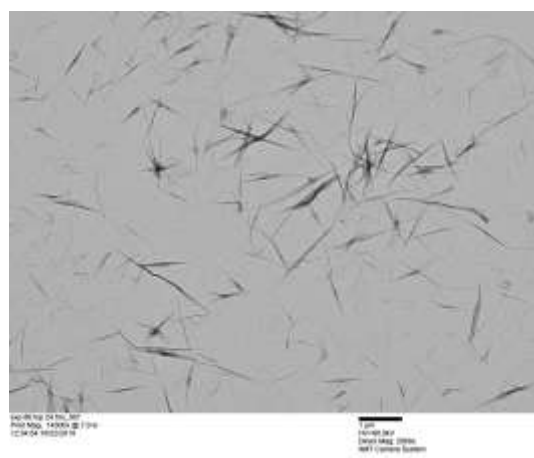


Figure 4.5: Trial 3, P3HT Nanoribbons (Scale bar 1 μ m)

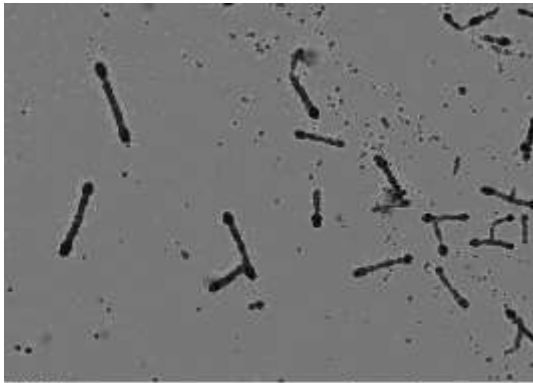


Figure 8.6: Trial 5, P3HT Nanorods
(Scale bar 1 um)

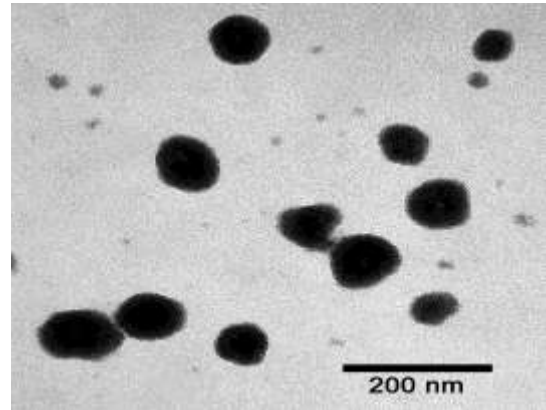


Figure 7.7: Trial 6, P3HT Nanoparticles
(Scale bar 200 nm)

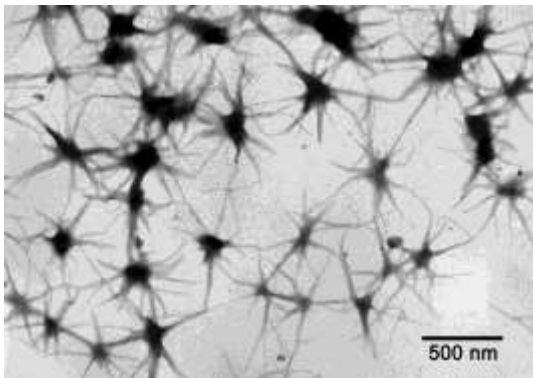


Figure 6.8: Trial 7, P3HT fibers
(Scale bar 500 nm)

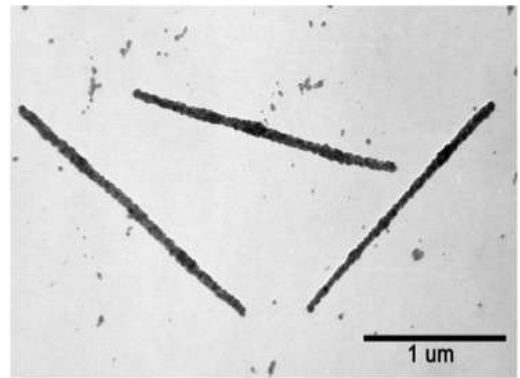


Figure 5.9: Trial 8, P3HT Nanorods
(Scale bar 1 um)

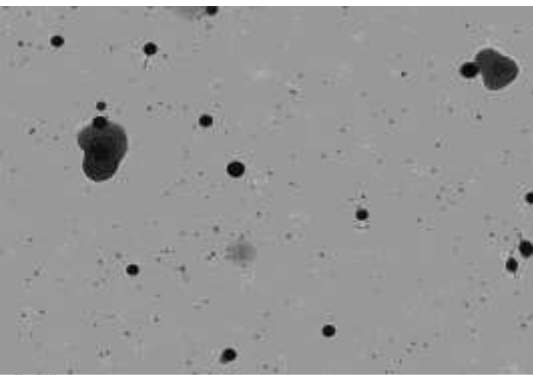


Figure 4.10: Trial 9, P3HT Nanoparticles
(Scale bar 600 nm)

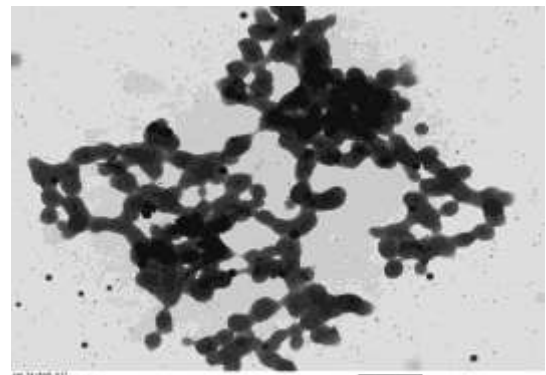


Figure 3.11: Trial 10, P3HT Nanoparticles
(Scale bar 1 um)

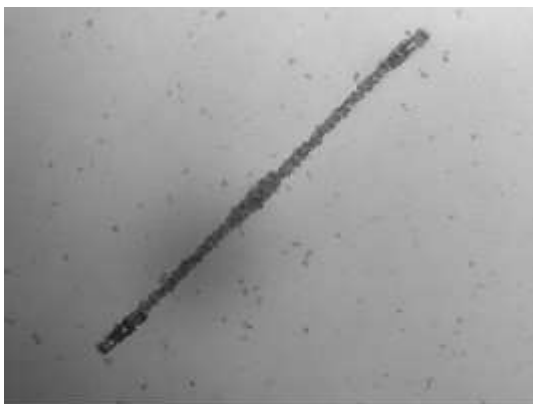


Figure 10.12: Trial 11, P3HT Nanorods
(Scale bar 600 nm)

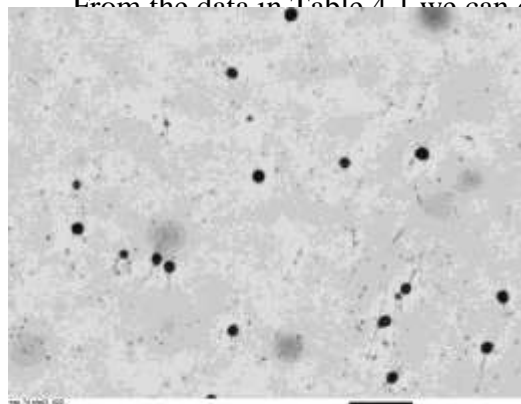


Figure 9.13: Trial 12, P3HT Nanoparticles
(Scale bar 600 nm)

nanorods in the solid rather than the supernatant.

CHAPTER 5

CONCLUSION

P3HT nanorods were successfully prepared using the modified Stöber Method. Different polymer nanostructures were obtained by varying the reaction conditions. The morphologies of these functionalized nanorods were examined using TEM and SEM. The nanorods were further characterized by FTIR. From the characterization of the nanorods, it is evident that the nanorods have been successfully synthesized, but there are some limitations that need to be addressed for future work. Some of the limitations include; morphology control, stability of the donor material, and its lifetime. The future work of this project will focus on optimizing the conditions to achieve higher power conversion efficiency and more stable morphology that will surpass the limitations of its long-term performance and efficiency. Upon completion of the project having addressed all the limitations, we hope that the cheaper and recyclable solar panels will help reduce the cost of OPVs and be affordable to the community. In the long run this may help reduce the energy cost and produce green energy technology.

REFERENCES

1. "Solar Energy Perspectives: Executive Summary" (PDF). International Energy Agency. 2011. Archived from the original on 2014-10-21.
2. Solar Fuels and Artificial Photosynthesis. Royal Society of Chemistry 2012 <http://www.rsc.org/ScienceAndTechnology/Policy/Documents/solar-fuels.asp> (accessed 21 October 2014)
3. Serway, R. A., *Physics for scientists & engineers*. Saunders College Pub.: 1990.
4. "Market Report 2013 (02)". *EPIA-publications*. European Photovoltaic Industry Association. March 2014. Archived from the original on 4 April 2014
5. Sunshot, Office of Energy Efficiency and Renewable Energy. U.S. Department of Energy. 2014. <http://energy.gov/eere/sunshot/about> (accessed 20 October 2014)
6. Organic Photovoltaics Research, Office of Energy Efficiency and Renewable Energy. U.S. Department of Energy. 2014. <http://energy.gov/eere/sunshot/organic-photovoltaics-research>
7. Ding B., Yu J. (2014). Electrospun Nanofibers for Energy and Environmental Applications. Springer. pp. 142-149.
8. "April 25, 1954: Bell laboratories Demonstrates the First Practical Silicon Solar Cell" *APS News* (American Physical Society) **18** (4). October 2014
9. D.M. Chapin, C.S. Fuller, and G.L. Pearson, A New Silicon p-n Junction Photocell for Converting Solar Radiation into Electrical Power, *J. Appl. Phys.* **25**, 676 (1954).
10. Rivers, P. N., *Leading edge research in solar energy*. Nova Science Publishers: 2007.
11. Sariciftci, N. S.; Smilowitz, L.; Heeger, A. J.; Wudl, F.; Photoinduced Electron Transfer from a Conducting Polymer to Buckminsterfullerene. *Science* **1992**, 258 (5087), 1474-1476.
12. Schnabel, W., *Polymers and Light: Fundamentals and Technical Applications*. John Wiley & Sons: 2007.
13. Liang, W Y (1970). "Excitons". *Physics Education* **5** (4): 226.
14. Winder, C.; Sariciftci, N. S., Low bandgap polymers for photon harvesting in bulk heterojunction solar cells. *Journal of Materials Chemistry* **2004**, 14 (7), 1077-1086.
15. McGehee, M. D.; Topinka, M. A., Solar cells: Pictures from the blended zone. *Nat Mater* **2006**, 5 (9), 675-676.
16. Hoppe, H.; Sariciftci, N. S., Organic solar cells: An overview. *Journal of Materials Research* **2004**, 19 (7), 1924-1945.

17. Kim, M. S.; Michigan, U. o., *Understanding Organic Photovoltaic Cells: Electrode, Nanostructure, Reliability, and Performance*. University of Michigan: 2009.
18. Hoppe, H.; Sariciftci, N. S., Morphology of polymer/fullerene bulk heterojunction solar cells. *Journal of Materials Chemistry* **2006**, 16 (1), 45-61.
19. Yam, V. W. W., *WOLEDs and Organic Photovoltaics: Recent Advances and Application*. Springer: 2010.
20. Halls, J. J. M.; Pichler, K.; Friend, R. H.; Moratti, S. C.; Holmes, A. B., Exciton diffusion and dissociation in a poly(p-phenylenevinylene)/C[₆₀] heterojunction photovoltaic cell. *Applied Physics Letters* **1996**, 68 (22), 3120-3122.
21. Kearns D., Calvin M. (**1958**). "Photovoltaic Effect and Photoconductivity in Laminated Organic Systems". *J. Chem. Phys.* **29** (4): 950–951.
22. Yang F. et al. (**2005**). "Controlled growth of a molecular bulk heterojunction photovoltaic cell". *Nature Materials* **4**: 37–41.
23. Stöber, W.; Fink, A.; Bohn, E., Controlled growth of monodisperse silica spheres in the micron size range. *Journal of Colloid and Interface Science* **1968**, 26 (1), 62-69.
24. Shiquan Liu et al., "Further Investigations on the Modified Stöber Method for Spherical MCM-41," *Materials Chemistry and Physics* 97, no. 2–3 (June 10, 2006): 203–6, doi:10.1016/j.matchemphys.2005.09.003.
25. Chi, D.; Qu, S.; Wang, Z.; Wand, J.; High efficiency P3HT:PCBM solar cells with an inserted PCBM layer. *J. Mater. Chem. C*, 2014, **2**, 4283.
26. Askari. Mohammad Bagher, "Introduction to Organic Solar Cells." *Sustainable Energy*, vol. 2, no. 3 (2014): 85-90. doi: 10.12691/rse-2-3-2.
27. Güneş, S.; Neugebauer, H.; Sariciftci, N.S.; Conjugated Polymer-Based Organic Solar Cells. *Chem. Rev.* **2007** 107, 1324-1338.
28. B. Neises, W. Steglich (1978). "Simple Method for the Esterification of Carboxylic Acids". *Angew. Chem. Int. Ed.* **17** (7): 522–524. doi:10.1002/anie.197805221
29. Hemali Rathnayake et al., "Synthesis and Characterization of poly(3-Hexylthiophene)-Functionalized Siloxane Nanoparticles," *Nanoscale* 5, no. 8 (March 28, 2013): 3212–15, doi:10.1039/C3NR34249B.
30. Stefan, M.C.; Javier, A.E.; Osaka, I.; McCullough, R.D., Grignard Metathesis Method (GRIM): Toward a Universal Method for the Synthesis of Conjugated Polymers. *Macromolecules* **2009** 42, 30-32.
31. Tamao, K.; Sumitani, K.; Kumuda, M., Selective carbon-carbon bond formation by cross-coupling of Grignard reagents with organic halides. Catalysis by nickel-phosphine complexes *Journal of the American Chemical Society* **1972** 94 (12), 4374-4376